Quantum walks on a random environment

Yue Yin, D. E. Katsanos, and S. N. Evangelou[*]

Department of Physics, University of Ioannina, Ioannina 45110, Greece
(Received 11 August 2007; published 5 February 2008)

Quantum walks are considered in a one-dimensional random medium characterized by static or dynamic disorder. Quantum interference for static disorder can lead to Anderson localization which completely hinders the quantum walk and it is contrasted with the decoherence effect of dynamic disorder having strength W, where a quantum to classical crossover at time $t_c \propto W^{-2}$ transforms the quantum walk into an ordinary random walk with diffusive spreading. We demonstrate these localization and decoherence phenomena in quantum carpets of the observed time evolution, we relate our results to previously studied models of decoherence for quantum walks, and examine in detail a dimer lattice which corresponds to a single qubit subject to randomness.

I. INTRODUCTION

During the last decade quantum algorithms were proposed, such as Grover's search [1] and Shor's factorization [2], which can in principle perform certain computational tasks quantum-mechanically, much more efficiently than their classical counterparts. The related idea of quantum walks was also introduced [3–7] which generalize the classical random walks widely used in various computations as the basis of classical algorithms. The quantum walks are similar to classical random walks but with a "quantum coin" operation which replaces the coin-flip randomness in between each moving step on a lattice or a graph. The state of the quantum coin which uniquely determines the subsequent movement direction can also exist in quantum superpositions, something impossible in the classical domain where the coin has a specific outcome. In analogy with classical random walks the quantum walks are expected to be useful for designing quantum algorithms. For example, Grover's algorithm can be combined with quantum walks in a quantum algorithm for "glued trees" which provides even an exponential speed up over classical methods [8].

The main advantage of quantum walks is a highly improved behavior over their classical counterparts since quantum wave propagation is superior to classical diffusion. For example, in the quantum case the ballistic mean square variance $\sigma^2(t) \propto t^2$ can be compared to the linear spread law $\sigma^2(t) \propto t$ of classical diffusion. This quadratic speed-up is a general feature of quantum search algorithms [1] and is also familiar from standard quantum evolution of tight-binding electron waves on a periodic lattice [9]. In quantum walks the classical probability $P(x,t)$ is replaced by complex probability amplitude $\Psi(x,t)$ computed from the unitary dynamics of the Schrödinger's equation. The corresponding probability amplitudes are determined by summing up over all possible paths of propagation. Furthermore, to describe wave propagation in lattices or graphs one does not need a "quantum coin," [10] and related continuous-time versions of quantum walks have been introduced [11]. The discrete and

continuous-time quantum walks have recently been related to Dirac and Schrödinger's equations, respectively [12].

We consider a continuous-time quantum walk via the equivalent problem of a quantum particle initially localized in a one-dimensional lattice, also in the presence of static or dynamic disorder. For a tight-binding electron at an integer lattice site labeled by x in one dimension at time t the wave function $\Psi(x,t)$ obeys the linear wave equation ($\hbar=1$)

$$\iota\partial\Psi(x,t)/\partial t = \epsilon(x,t)\Psi(x,t) + \Psi(x-1,t) + \Psi(x+1,t), \quad (1)$$

with $\epsilon(x,t)$ an x-dependent random variable for static disorder which is also t-dependent for dynamic disorder, where lengths are measured in units of the lattice spacing and energies or inverse times in units of the hopping integral. In order to study quantum walks via Eq. (1) we choose the initial condition of a particle at the origin $x=0$ with $\Psi(x,t=0)=\delta_{x,0}$ and characterize the quantum motion by the second moment for its position $\sigma^2(t)=\Sigma_x|x|^2 P(x,t)$, where $P(x,t)=|\Psi(x,t)|^2$ is the probability density. In the absence of disorder [$\epsilon(x,t)=0$] the amplitude is given by the Bessel function so that $P(x,t)=[J_x(2t)]^2$, where the order x of the Bessel function measures the distance traveled from the origin while its argument is proportional to time t. The evolution of the wave packet at time t was shown [9] to display two sharp ballistic fronts at $x=\pm 2t$. From properties of the Bessel functions inside the spatial region $[-2t, 2t]$ the probability density $P(x,t)$ is an oscillating function multiplied by $1/t$ while outside this region, denoted by the two ballistic peaks, $P(x,t)$ decays exponentially. The ballistic mean-square displacement is $\sigma^2(t)=2t^2$.

In the absence of disorder the quantum evolution of wave packets which occurs via the evolution operator $\exp(-iHt)$ with Hamiltonian H is very different from classical diffusion where any initial state converges to a Gaussian steady state. An initially squeezed δ-function spatial wave packet has reduced spatial uncertainty and behaves like a quantum particle consisting of all the eigenstates of H. Alternatively, a spatially uniformly distributed initial wave packet $\Psi(x,0)=1/\sqrt{N}$, for every x in an N-site chain, consists of few eigenstates of H near the lower band edge only. Since the latter choice emphasizes states from the band edge the semiclassi-

*sevagel@cc.uoi.gr

cal asymptotics is relevant [13–15]. The wave packets which initially consist of many eigenstates can be related via the uncertainty principle to ultrashort laser pulses of femtosecond duration. The evolution of such coherent superpositions of quantum states is realized in the physics of trapped atoms in optical lattices [16], trapped ions [17], etc.

Classical random walks in perfect one-dimensional lattices are defined by the probabilities $p_x = q_x = 1/2$ which determine the left and right random motion starting from site x. This externally induced randomization leads to classical diffusion for long t with a Gaussian $P(x,t)$ and $\sigma^2(t) = 2Dt$, D the diffusion coefficient. For random walks in random media the probabilities $p_x, q_x = 1 - p_x$ become random variables themselves, for example, they could be chosen from a flat distribution within (0, 1). Then, this is the so-called random or Sinai walk [18,19] which leads to ultraslow classical evolution $\sigma^2(t) \propto \ln^4 t$, very close to a complete cease.

The problem addressed in this paper concerns the fate of quantum walks in a random environment with static and dynamic disorder. To answer this question for static disorder we shall combine previous knowledge from the field of wave propagation in the presence of randomness where the quantum phenomenon of Anderson localization [20] takes place (for its consequences for quantum walks see [21]). We shall show that static disorder is responsible for exponentially suppressed quantum evolution with variance $\sigma^2(t)$ reaching a time-independent limit for long t, depending on the strength of static disorder and space dimensionality. There are certain exceptions to this rule, for example, for correlated static disorder the obtained time evolution, although slower than ballistic (sub-ballistic), is superdiffusive $\sigma^2(t) = 2t^{3/2}$, due to resonances occurring even in one dimension [22]. Generalizations of discrete-time quantum walks in aperiodic or fractal media by using biased quantum coins have also given slower (sub-ballistic) quantum evolution [23]. Surprisingly, classical random walks for static disorder are still propagating, although ultraslowly [18,19]. For dynamic disorder by coupling the quantum system to a random environment decoherence occurs [24] and quantum physics becomes classical so that a quantum walk is still propagating but only diffusively. The effects of decoherence are considered in Ref. [25] where nonunitary evolution is modeled by computing density matrix operators. It was pointed out (see also [26]) that possibilities exist of tuning quantum walks with small values of added randomness. The quantum ballistic motion remains although the distribution itself becomes a uniform "top-hat," which optimizes properties of quantum walks useful for algorithms.

The main reason for examining the robustness of quantum walks in the presence of noise is because disorder is unavoidable in most quantum systems. Static disorder also appears for electrons in lattices with permanent modifications due to impurities. The dynamic disorder in this case could be driven by time-dependent vibrations of the lattice atoms and these have an impact on the electronic site-energies. Apart from describing electron-phonon interactions, dynamic disorder also addresses the presence of time-dependent noise in the memory qubits of quantum computers. Recently, qubit decoherence has attracted attention [27] in the presence of non-Gaussian noise from random flips of bistable fluctuators.

We demonstrate that although static disorder hinders the motion of quantum walks due to destructive quantum interference from Anderson localization via multiple scattering from impurities, instead, for a simple dynamically random environment, the time-dependent disorder acts as a decoherence mechanism at a crossover time t_c which randomizes the quantum walks and turns the quantum motion into classical. The discrete finite space chosen in the simulations could be also used on a finite computer. This general scheme for discretizing space is not only suggested by solid state applications but it is, somehow, related to the discreteness of the quantum information itself. The paper is organized as follows: In Sec. I we introduced the reader to the subject of quantum communication by setting the aims of our quantum walk in random media simulation. In Sec. II we briefly review the properties of quantum walks in ballistic and disordered one-dimensional media by showing quantum carpets which demonstrate the difference between static and dynamic disorder. Static disorder is shown to be responsible for destructive quantum interference of Anderson localization which stops completely the quantum walk while dynamic disorder permits only diffusive evolution of classical random walks. In Sec. III we display the quantum to classical crossover for dynamic disorder and consider a qubit subject to dynamic disorder. Finally, in Sec. IV we summarize our main conclusions.

II. QUANTUM CARPETS

We have created space-time $x-t$ structures for the probability density $P(x,t)$ on a one-dimensional finite N-site orthonormal lattice space without disorder, with t-independent static disorder and also rapidly varying dynamic disorder. The white color in the figures denotes high probability density and the darker colors lower values. In Fig. 1 a state is initially released in the middle of the chain and the probability density $P(x,t)$ is obtained by solving Eq. (1). In Fig. 2 the same is done for a spatially uniform initial state. For static disorder Eq. (1) could be alternatively solved by considering the time-evolution of a state vector $|\Psi(0)\rangle$ expressing the probability density via the stationary eigensolutions $H|j\rangle = E_j|j\rangle$ with space-time wave function

$$\Psi(x,t) = \sum_{j=1}^{N} e^{-iE_j t} \psi_j(x) \langle j|\Psi(0)\rangle, \qquad (2)$$

with the amplitude on site x denoted by $\psi_j(x) = \langle x|j\rangle$. For time-dependent disorder Eq. (1) was solved via a fourth-order Runge-Kutta algorithm.

In Fig. 1 we present our results for the initial choice of a δ function in the middle of the chain with $|\Psi(0)\rangle = |0\rangle$ and in Fig. 2 for a uniform initial state $|\Psi(0)\rangle = (1/\sqrt{N})\Sigma_{x=1}^{N}|x\rangle$ is computed on finite chains where the wave packet scatters from their hard ends. In Figs. 3–7 our results are obtained for a self-expanding chain with a δ function initial choice to make sure that the wave packet does not reach the boundaries. This allows one to study the quantum to classical crossover by computing the mean-square variance and the autocorrelation function vs time.
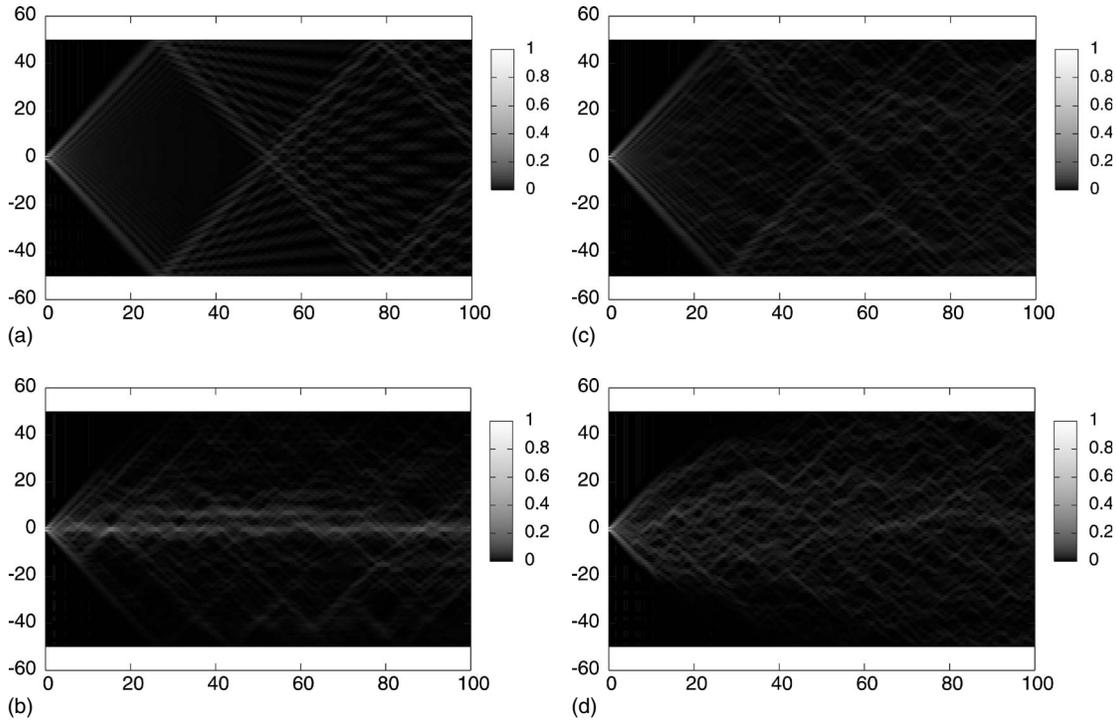
FIG. 1. Quantum carpets which show the probability density $P(x,t)$, for x in the vertical axis and t in the horizontal axis, is generated by an initial δ-type spatial state for $t=0$ $\Psi(x,0)=\delta_{x,0}$ in the middle (left of the figure) with chain length $N=101$. (a) The ballistic case for the absence of disorder where perfect quantum revivals can be clearly seen. (b) For static disorder of strength $W=1.5$ quantum interference causes Anderson localization which stops the quantum motion and the probability to stay in the initial site remains high. For stronger static disorder this probability becomes even higher. (c) and (d) For dynamic disorder with values $W=1$ and 5, one can see quantum interference only initially for small t on the left-hand side of the figure where the δ-type wave packet moves ballistically. After a certain time (for $W=1$, $t_c \approx 60$ is estimated and for $W=5$ about $t_c \approx 3$) the quantum interference is lost while the particle still moves but classically.

A. Ballistic motion

In this case, obviously, quantum walks perform at their best. The ballistic description is valid for solid state systems in the absence of disorder refering to the motion of a point particle in an N-site chain with $\epsilon=0$ in Eq. (1) which gives $E_j=2\cos\left(\frac{\pi j}{N+1}\right)$ and $\psi_j(x)=\sqrt{\frac{2}{N+1}}\sin\left(\frac{j\pi x}{N+1}\right)$, $j=1,2,\ldots,N$. The corresponding space-time pictures are shown in Figs. 1(a) and 2(a) where quantum revivals can be seen where the particle returns to its initial position and reconstructs like a classical particle which moves with constant velocity reflecting at the boundaries of the chain [15]. We observe that the quantum revivals of Figs. 1(a) and 2(a) do not repeat indefinitely but become less and less accurate as time progresses. This is due to effects from boundary scattering which is more intense for broad wave packets as seen in the right-hand side of Fig. 2(a) where noisy evolution is established. The obtained fractal pattern is a result of peculiar quantum interference effects due to scattering from the hard walls at the ends of the chain [15].

B. Static disorder

It can have dramatic consequences for quantum walks, particularly in low dimensions, since for static disorder they can stop completely due to Anderson localization. From Figs. 1(b) and 2(b) we can see how strong static disorder

with $\epsilon(x)$ chosen from a uniform probability distribution within $[-W/2,+W/2]$ causes destructive interference with Anderson localization. This crossover from ballistic motion to localization has dramatic consequences for quantum walks in one-dimension in the presence of static disorder. In higher dimensions the Anderson transition from extended to localized states is expected, via an intermediate chaotic regime which is rather better for quantum propagation. The probability density of Fig. 1(b) is shown to stay around the middle site where the initial wave packet has maximum amplitude and it remains there for longer times. For the uniform initial state of Fig. 2(b) the larger amplitudes remain on many sites indefinitely.

C. Dynamic disorder

A quantum walk can operate in the presence of dynamic disorder but only for short times since for longer times its motion becomes entirely classical, indistinguishable from an ordinary random walk. The effect of dynamic disorder is equivalent to introducing coin chaos which makes the quantum coherence disappear [24–26]. Although the chosen noise is simpler a lot of interest exists in non-Gaussian noise [27]. In order to see this decoherence effect we have chosen a random $\epsilon(x,t)$ rapidly varying with t by

(i) updating at random the diagonal site energies $\epsilon(x,t)$ at a time length comparable and often much smaller to the time step of the numerical method; and
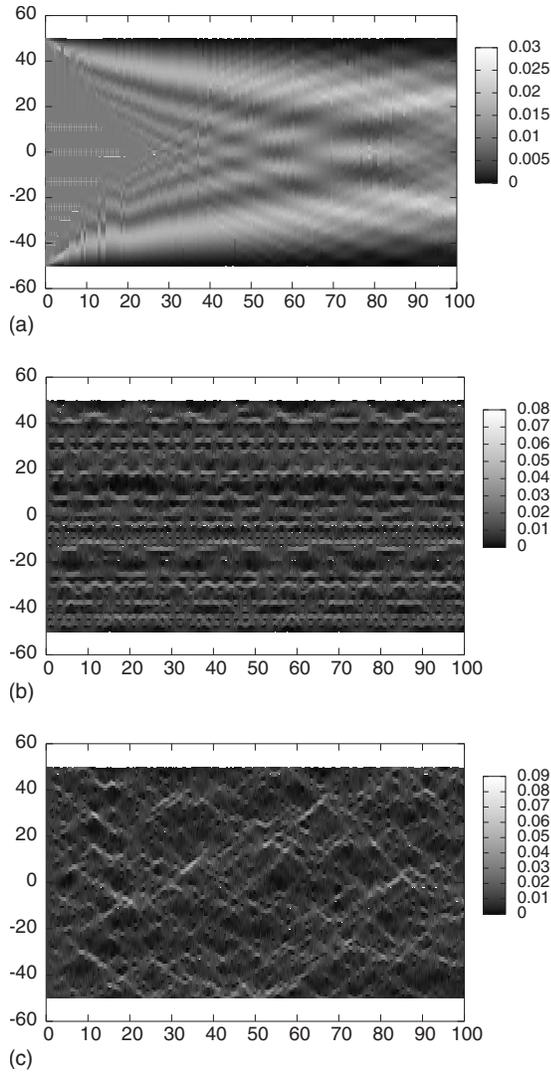
(a)

(b)

(c)

FIG. 2. Quantum carpets showing the probability density $P(x,t)$ for a spatially uniform initial state $\Psi(x,0)=1/\sqrt{N}$ on a chain of length $N=101$. (a) For the ballistic case in the absence of disorder one can see recurrences for short times which disappear for longer times where quantum interference effects become apparent. (b) For static disorder of strength $W=5$ Anderson localization occurs with localization length $\xi \sim 100W^{-2} \sim 4$ much less than the system size $N=101$. The displayed regions of high amplitudes show the positions where the particle localizes. (c) In the presence of dynamic disorder $W=5$ the quantum interference effects vanish. The main difference between dynamic disorder (c) and static disorder (b) is that in (c) the regions with high values of $P(x,t)$ keep changing leading to randomization so that the particle can still move but in a "classical" fashion.

(ii) varying the diagonal energies by

$$\epsilon(x,t) = A \cos(\omega_x t + \phi_x), \tag{3}$$

where A, ω, and ϕ are the amplitude, frequency, and phase for the motion of levels, respectively. We chose to vary the frequency ω at random uniformly within the interval $[0, 2\pi]$ and fixed the phase ϕ_x to zero.
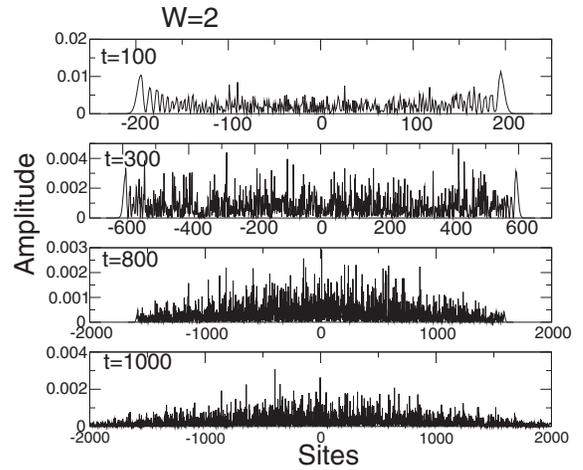

FIG. 3. The probability density is shown to display the gradual decoherence, from ballistic for small t to diffusive evolution for long t, with strength of dynamic disorder $W=2$. The two ballistic fronts in the quantum case gradually disappear and the shape approaches a Gaussian with classical diffusion.

From Figs. 1(c), 1(d), and 2(c), we can see the effect of dynamic disorder for the two initial wave packets, δ function, and broad, respectively. In Fig. 1(c) the quantum motion seen on the left-hand side of the figure quickly disappears and this also happens in Fig. 1(d) where classical
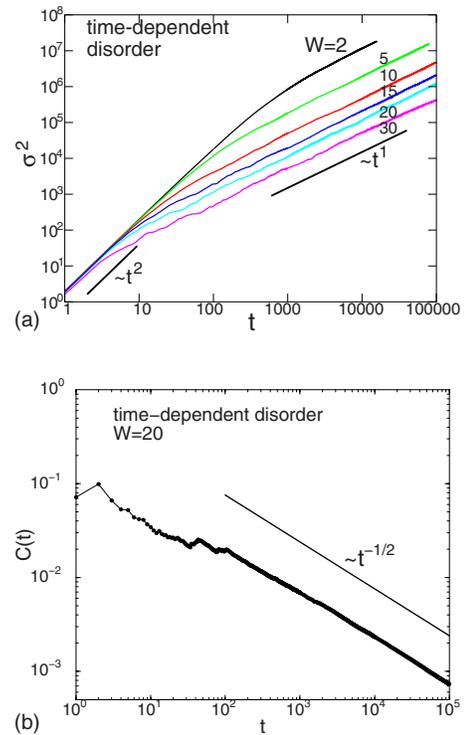

(a)

(b)

FIG. 4. (Color online) (a) Log-log plot of the mean-square displacement or variance $\sigma^2(t)$ vs time t for various values for the dynamic disorder W. The crossover from ballistic quantum motion to diffusive classical motion occurs at earlier times as W increases. (b) The autocorrelation function or "return to the origin" probability $C(t)$ vs t for $W=20$ displays classical diffusive behavior.
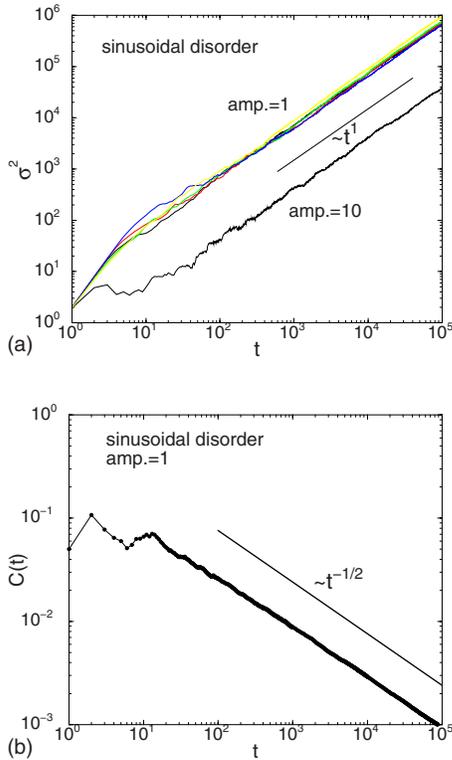
FIG. 5. (Color online) (a) The $\sigma^2(t)$ vs time t the same as in Fig. 4(a) but for the sinusoidal dynamic disorder of Eq. (4). (b) The $C(t)$ vs time t the same as in Fig. 4(b) but for the sinusoidal dynamic disorder of Eq. (4).

diffusive motion is seen to arise. In Fig. 2(c) the randomization effects of dynamic disorder become more obvious and could be contrasted with quantum localization for static disorder [Fig. 2(b)]. The quantum-to-classical crossover takes place after a characteristic time $t_c \propto W^{-2}$.

III. QUANTUM TO CLASSICAL CROSSOVER FOR DYNAMIC DISORDER

A. Decoherence in an N-site chain

The decoherence effect of dynamical disorder which turns the quantum wave propagation into classical diffusion is shown in Fig. 3 for a self-expanding chain. The probability density $P(x,t)$ gradually changes from a shape displaying two ballistic peaks of the quantum wave for small t towards a Gaussian for large t. In Fig. 4 the quantum to classical crossover is shown for the mean-square-variance $\sigma^2(t)$ and the autocorrelation function or return probability $C(t) = \frac{1}{t}\int_0^t P(0,t')dt'$. Eventually, the classical asymptotic laws $\sigma^2(t) \propto t$ and $C(t) \propto t^{-1/2}$ set in after an initial period of quantum ballistic motion where $\sigma^2(t) \propto t^2$ and $C(t) \propto t^{-1}$. In Fig. 5 the effect of sinusoidal dynamic disorder is considered with constant amplitude and randomly varying the phase. The results are similar to Fig. 4 with the approach to the classical limit even faster in this case. From Figs. 4 and 5, except for no difference between the two types of dynamic disorder, we find that the crossover region between the ballistic law for
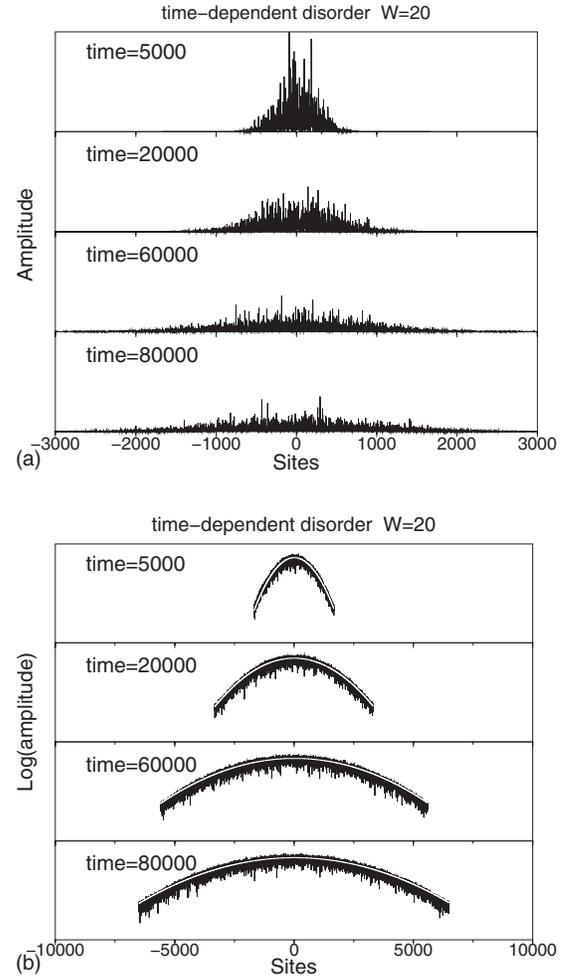

FIG. 6. The snapshots for dynamic disorder of strength $W=20$ in a self-expanding chain where the approach to a Gaussian is seen. (a) The probability density $P(x,t) = |\Psi(x,t)|^2$ as a function of space x at fixed times $t=5000$, 20 000, 60 000, and 80 000. (b) The same as in (a) but for the log of the amplitude.

small times and the diffusive law for long times is smooth having a mixed quantum and classical character.

The effect of dynamic disorder on the quantum evolution is displayed in the linear and log plots of Fig. 6 which show the snapshots of the evolving spatial wave for an initial δ function in a self-expanding chain. The decoherence effect of dynamical disorder is seen from the rapid approach to a Gaussian shape. The complete phase diagram is summarized in Fig. 7 with t_c vs the strength of dynamic disorder W which displays a wide crossover gray color region where the law $t_c \propto W^{-2}$ is approximately obeyed.

B. Decoherence in a qubit

We have examined in detail the quantum walk in a random two-level system ($N=2$) which has recently attracted attention in the context of quantum information processing. The operation of qubit and logical gates in the presence of a noisy environment is important for understanding quantum computers. The usual noise for such a two-level system is
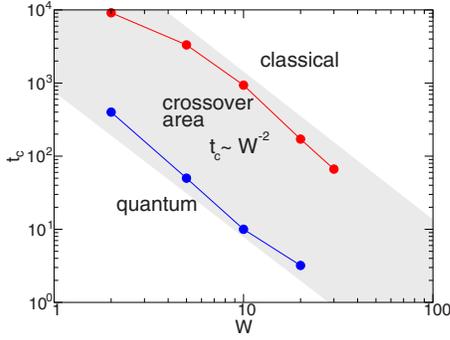
FIG. 7. (Color online) The quantum to classical crossover for dynamic disorder of strength W occurs at $t_c \propto W^{-2}$. This is shown by the gray area which was estimated from two sets of points connected via lines for the quadratic ballistic law to stop (blue, lower line) and the linear diffusive law to begin (red, upper line), respectively.
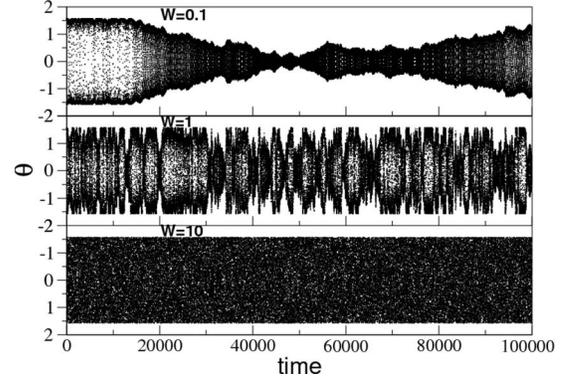

FIG. 8. The phase θ of the off-diagonal matrix element of the density matrix $\rho_{1,2}$ vs time for a two-level system with dynamic disorder $W=0.1$, 1, and 10. The decoherence due to dephasing is seen for the highest value $W=10 > W_c$ where θ completely randomizes.

usually due to various sources while non-Gaussian randomness arises from hopping background charges for different statistically independent fluctuators [27].

The time-dependent Hamiltonian is

$$H = \begin{pmatrix} \epsilon_1(t) & \gamma \\ \gamma & \epsilon_2(t) \end{pmatrix}, \tag{4}$$

with random diagonal terms defined by

$$\langle \epsilon_i(t) \rangle = 0, \quad \langle \epsilon_i(t)\epsilon_j(t') \rangle = \delta \delta_{i,j} \delta(t-t'), \quad i,j=1,2, \tag{5}$$

where $\delta = W^2/12$ measures the disorder chosen from a box distribution within $[-W/2, +W/2]$. The averaged matrix elements of the density matrix ρ can be obtained from a decoupling suggested in [28]

$$\iota \overline{\dot{\rho}_{11}} = -\iota \overline{\dot{\rho}_{22}} = \gamma(\overline{\rho_{21}} - \overline{\rho_{12}}), \tag{6}$$

$$\iota \overline{\dot{\rho}_{12}} = -2\iota \delta \overline{\rho_{12}} + \gamma(\overline{\rho_{22}} - \overline{\rho_{11}}), \tag{7}$$

and if we define

$$\overline{\rho_{11}} = \frac{1}{2} + \rho, \quad \overline{\rho_{22}} = \frac{1}{2} - \rho, \quad \overline{\rho_{12}} = R + iJ, \quad \overline{\rho_{21}} = R - iJ, \tag{8}$$

the corresponding equations become

$$\dot{\rho} = -2\gamma J, \quad \dot{R} = -2\delta R, \quad \dot{J} = -2\delta J + 2\gamma\rho. \tag{9}$$

It must be emphasized that these equations describe qubit dephasing which was considered before for quantum walks on a hypercube [24]. Their general solutions (with appropriate constants) are

$$\begin{pmatrix} \rho \\ J \end{pmatrix} = C_+ \begin{pmatrix} -2\gamma \\ \Lambda_+ \end{pmatrix} e^{\Lambda_+ t} + C_- \begin{pmatrix} -2\gamma \\ \Lambda_- \end{pmatrix} e^{\Lambda_- t}, \tag{10}$$

$$R = C_R e^{-2\delta t}, \quad \Lambda_\pm = -\delta \pm \sqrt{\delta^2 - 4\gamma^2}, \tag{11}$$

by choosing as the initial state one of the two levels with $\rho(0)=1/2$, $R(0)=J(0)=0$.

Finally, the averaged off-diagonal matrix element of the density matrix can be easily shown to be

$$\overline{\rho_{12}(t)} = \iota J(t) = \frac{\iota \gamma}{\sqrt{4\gamma^2 - \delta^2} -} \sin(\sqrt{4\gamma^2 - \delta^2}t)e^{-\delta t} \tag{12}$$

for $\delta^2 < 4\gamma^2$. If $\delta^2 > 4\gamma^2$ in Eq. (12) the quantity under the square root changes sign and sin is replaced by sinh. Thus for $t \to \infty$ the averaged density matrix approaches half the unit matrix with only diagonal matrix elements and the quantum coherences described by $\overline{\rho_{12}}$ becoming zero, oscillating for the quantum case $\delta < 2\gamma$ and monotonically decaying for the classical case $\delta > 2\gamma$.

In order to examine the dephasing effect of dynamic disorder we have plotted in Fig. 8 the phase θ of $\rho_{1,2}$ vs t obtained from numerical computations without averaging. Our results are presented for $\gamma=1$ and different values of disorder W which verify the critical value $W_c = \sqrt{24}$ of the previous analysis based on averages. The quantum coherence remains for weak dynamic disorder $W < W_c$ while for higher dynamic disorder $W > W_c$ the phase randomizes and the system becomes classical.

IV. DISCUSSION

Quantum walks are quantum analogs of classical random walks which have been proposed in order to create quantum algorithms which run faster in quantum computers. They can also arise from mapping various physical problems (see, e.g., [29]). Some quantum algorithms which speed-up classical methods have already been successfully employed, such as for search problems on graphs. These algorithms which show amplitude amplification during the evolution could be efficiently implemented in a quantum computer. However, since they are often confronted with disorder we have examined how quantum wave packets move in the presence of disorder

by computing the probability density $P(x,t) = |\Psi(x,t)|^2$ from solving the time-dependent Schrödinger equation in the discrete space x of a one-dimensional lattice. The static disorder is due to imperfections and the dynamic disorder could be due to the environment which might become obvious in scattering from nanostructures, averaging over measurements, etc.

Our main conclusions from the quantum evolution of the δ function and very broad initial spatial wave packets are as follows. (1) In random media quantum walks often perform worse than their classical counterparts since destructive quantum interference leads to Anderson localization which completely stops the quantum walk although the corresponding ordinary random walks in the presence of disorder can still move infinitely slowly. (2) For dynamic disorder we have no benefit from quantum walks either, since the ballistic evolution for small-t crosses over to classical diffusion for long-t and the quantum walks become classical via a quantum to classical crossover. (3) The answer to the question "what slows down a quantum walk?" is, on one hand, "static

disorder via destructive quantum interference" and, on the other hand, "dynamic disorder which makes the quantum walk at long enough times no different from ordinary random walk." Therefore quantum interference in random media can hold surprises for quantum walks and their advantages appear for weak disorder or short times only. In higher dimensions quantum walks are also expected to operate but for weak disorder only in order to avoid quantum localization. The fact that a small amount of decoherence can be beneficial for quantum walks by making the distributions more uniform is also expected to appear after averaging since the problem reduces to previous decoherence studies [24], as it was shown in Sec. III for a single qubit. In conclusion, our computations show Anderson localization or decoherence as the main enemies of quantum walks in the presence of static and dynamic disorder, respectively, which destroy their well-known quadratic or exponential speed-up. Our study could be useful towards creating better quantum search algorithms in the presence of disorder [30].

---

[1] L. K. Grover, Phys. Rev. Lett. **79**, 325 (1997).

[2] P. W. Shor, SIAM J. Comput. **26**, 1184 (1997).

[3] Y. Aharonov, L. Davidovich, and N. Zagury, Phys. Rev. A **48**, 1687 (1993).

[4] D. A. Meyer, J. Stat. Phys. **85**, 551 (1996).

[5] E. Farhi and S. Gutmann, Phys. Rev. A **58**, 915 (1998).

[6] For an introductory review to *quantum random walks* see: J. Kempe, Contemp. Phys. **44**, 307 (2003).

[7] A. Ambainis, Int. J. Quantum Inf. **1**, 507 (2003).

[8] A. M. Childs, R. Cleve, E. Deotto, E. Farhi, S. Gutmann, and D. A. Spielman, *Proceedings of the 35th ACM Symposium on Theory of Computing* (ACM Press, San Diego, 2003), p. 59.

[9] D. E. Katsanos, S. N. Evangelou, and S.-J. Xiong, Phys. Rev. B **51**, 895 (1995).

[10] A. Patel, K. S. Raghunathan, and P. Rungta, Phys. Rev. A **71**, 032347 (2005).

[11] A. M. Childs, E. Farhi, and S. Gutmann, Quantum Inf. Process. **1**, 35 (2002).

[12] F. W. Strauch, Phys. Rev. A **74** 030301(R) (2006); **73** 054302 (2006).

[13] M. V. Berry, J. Phys. A **26**, 6617 (1996).

[14] M. Berry, I. Marzoli, and W. Schleich, Phys. World **14**, 39 (2001).

[15] I. Amanatidis, D. E. Katsanos, and S. N. Evangelou, Phys. Rev. B **69**, 195107 (2004).

[16] W. Dur, R. Raussendorf, V. M. Kendon, and H.-J. Briegel, Phys. Rev. A **66**, 052319 (2002).

[17] B. C. Travaglione and G. J. Milburn, Phys. Rev. A **65**, 032310 (2002).

[18] Ya. G. Sinai, Theor. Probab. Appl. **27**, 247 (1982).

[19] J. P. Bouchaud and A. Georges, Phys. Rep. **195**, 127 (1990).

[20] P. W. Anderson, Phys. Rev. **109**, 1492 (1958).

[21] J. P. Keating, N. Linden, J. C. F. Matthews, and A. Winter, Phys. Rev. A **76**, 012315 (2007).

[22] D. H. Dunlap, H.-L. Wu, and P. W. Phillips, Phys. Rev. Lett. **65**, 88 (1990); P. Phillips and H.-L. Wu, Science **252**, 1805 (1991).

[23] P. Ribeiro, P. Milman, and R. Mosseri, Phys. Rev. Lett. **93**, 190503 (2004).

[24] V. Kendon, e-print arXiv:quant-ph/0606016.

[25] V. Kendon and B. Tregenna, Phys. Rev. A **67**, 042315 (2003).

[26] O. Maloyer and V. Kendon, New J. Phys. **9**, 87 (2007).

[27] Y. M. Galperin, B. L. Altshuler, J. Bergli, and D. V. Shantsev, Phys. Rev. Lett. **96**, 097009 (2006).

[28] A. A. Ovchinikov and N. S. Erikhman, Sov. Phys. JETP **40**, 733 (1975).

[29] T. Oka, N. Konno, R. Arita, and H. Aoki, Phys. Rev. Lett. **94**, 100602 (2005).

[30] P. Shor, Quantum Inf. Process. **3**, 5 (2004).